The "Power Network" of Genetic Circuits

Yili Qian and Domitilla Del Vecchio

1 Introduction

Synthetic biology is an emergent research field whose aim is to engineer novel genetic circuits in living cells. It has potential applications ranging from increasing biofuel production [25], to sensing environmental hazards [2], and to detecting and/or killing cancer cells [8, 9]. Enabled by advancements in genetic engineering, ever since early 2000s, researchers have been able to construct simple genetic circuits, often with no more than two or three genes, that can achieve certain functionalities. These functional circuits include, for instance, genetic toggle switches [16], genetic oscillators [14] and transcriptional negative feedback loops [31]. They were built with the purpose to deepen our understanding of natural systems and to demonstrate current engineering capabilities. Stimulated by the need for cells with sophisticated sensing, computing and actuation capabilities, in recent years, there has been a transition in the field towards engineering large scale and complex genetic systems [4, 26]. However, such efforts are often impeded by context dependence, the fact that functional genetic modules behave differently when they are connected in a circuit as opposed to when they are in isolation. In particular, many synthetic circuits fail due to unintended interactions among genes and with the cellular "chassis"[6]. Context dependence often leads to lengthy and *ad-hoc* design processes with unpredictable outcomes, largely hindering our capability to scale up genetic circuits for real-world applications. Therefore, much of the current research in the field is devoted to the mitigation of context dependence in genetic circuits, with the aim to robustify and modularize them [10]. These research questions can

Yili Qian
Department of Mechanical Engineering, Massachusetts Institutie of Technology. e-mail: yiliqian@mit.edu

Domitilla Del Vecchio
Department of Mechanical Engineering and Synthetic Biology Center, Massachusetts Institutie of Technology. e-mail: ddv@mit.edu

be formulated as classical systems and control theory problems such as disturbance attenuation, output regulation and reference tracking [11]. However, their solutions are often challenged by physical constraints in living cells (see [11] for a comprehensive review on the application of control theory to synthetic biology). One successful engineering example is the mitigation of "retroactivity", where the unintended loading from a downstream genetic module to its upstream module can be mitigated through engineered biomolecular insulation devices [13, 23, 24].

In this paper, we review our latest research outcomes on the modeling, analysis and mitigation of another form of context dependence that has received much attention recently: the competition among synthetic genes for a limited amount of cellular resources provided by the host cell [5, 7, 17, 28, 30].

Gene expression *in vivo* relies on the key processes of transcription and translation. Transcription is initiated by RNA polymerases (RNAPs) binding with the promoter sites of DNAs to produce messenger RNAs (mRNAs), which are then translated by ribosomes to produce target proteins. Genetic circuits are gene regulatory networks (GRNs) that are constructed by allowing transcription of one gene to be regulated by proteins expressed by other genes. These proteins are called transcription factors (TFs), which can either activate or repress transcription by binding with promoter sites on DNAs (see Figure 1A). Therefore, naturally, the functionality of any GRN requires the availability of RNAPs and ribosomes [12].

Recent experimental results have suggested that the limited amount of ribosomes is the main bottleneck for gene expression in *E. coli* bacteria in exponential growth phase [17, 19]. Competition for ribosomes can create hidden interactions among genes: activating production of protein A reduces the amount of resources available to produce protein B. In particular, it has been demonstrated experimentally that due to resource competition, expression of an unregulated gene can be reduced by more than 60% when expression of another gene is activated [5, 17]. Similar phenomena have been observed in cell-free systems [32] and in computational models [22, 30]. However, resource limitation is often neglected in standard gene expression models [1, 12], and rarely considered in circuit design, leading to unexpected design outcomes. Therefore, it is desirable to develop a systematic framework to model and mitigate the effects of resource competition in genetic circuits.

In this paper, we provide a review of our recent progress toward these goals [27, 28, 29]. In [27, 28], we developed and experimentally validated a general gene expression model accounting for resource competition. These results are briefly reviewed in Section 2 and Section 3. In Section 4, we review our recent theoretical work on mitigating the effects of resource competition by introducing a system concept and formulating the problem as a disturbance decoupling problem for networks [29]. The problem can be solved by implementing decentralized feedback controllers described in Section 5. Section 6 discusses the stability of the decentralized control scheme. Simulation examples are provided in Section 7.

2 Modeling resource competition in gene networks

A GRN is an interconnection of gene expression cassettes, which we call *nodes*. Each node i takes l_i TFs as inputs to regulate the production of a TF $\mathrm{x_i}$ as output (Figure 1A). We denote the set of TF inputs to node i by $\mathcal{U}_i$ (see Figure 1B), and use $\mathbf{u}_i = [u_1, \cdots, u_{l_i}]^T$ to represent their concentrations. A series of chemical reactions take place in a node. The input TFs to node i can bind with the DNA promoter site in node i to either activate or repress its ability to recruit RNAPs to produce mRNA $\mathrm{m_i}$; free ribosomes then bind with mRNAs to initiate translation and produce output TF $\mathrm{x_i}$. Assuming that binding reactions are much faster than transcription and translation [1, 12], the state of each node can be described by the concentrations of its mRNA transcript m_i and TF output x_i (*italics*). In a standard gene expression model [1, 12], the free amount of ribosomes available for translation is often assumed to be constant, yielding the following node dynamics:

$$\dot{m}_i = T_i F_i(\mathbf{u}_i) - \delta_i m_i, \qquad \dot{x}_i = R_i m_i - \gamma_i x_i, \tag{1}$$

where T_i is the maximum transcription rate constant, R_i is the translation rate constant proportional to the free concentration of ribosomes, and δ_i and γ_i are the mRNA and protein decay rate constants, respectively. The function $F_i(\mathbf{u}_i)$ describes transcriptional regulation of the input TFs on node i, and can be written as a standard Hill function [1, 12]. Based on reaction rate equations, when node i takes a single TF input whose concentration is u_i, the Hill function $F_i(u_i)$ takes the following form [12]:

$$F_i(u_i) = \begin{cases} \frac{\beta_i + (u_i/k_i)^{n_i}}{1+(u_i/k_i)^{n_i}}, & \text{if } \mathrm{u_i} \text{ is an activator} \\ \frac{1}{(u_i/k_i)^{n_i}}, & \text{if } \mathrm{u_i} \text{ is an activator,} \end{cases} \tag{2}$$

where k_i is the dissociation constant of TF $\mathrm{u_i}$ binding with the promoter site of node i. The stronger the binding affinity, the smaller the dissociation constant. Parameter n_i is the binding Hill coefficient, and $\beta_i \in [0,1)$ characterizes basal expression (i.e. expression when $u_i = 0$). In a GRN, nodes are connected through regulatory inter-

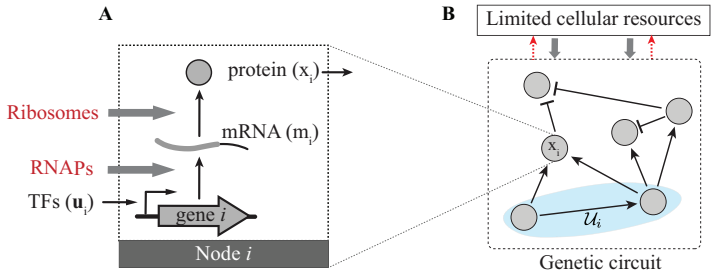

Fig. 1 (A): Schematic of gene expression process in a node i. (B): In a GRN, all nodes are competing for a limited amount of resources in the host cell.

actions, where the output of node i ($\mathrm{x_i}$) can be a TF input to either activate or repress gene expression in other nodes. In a GRN composed of n nodes, let $\mathbf{x} = [x_1, \cdots, x_n]^T$ represent the concentrations of all TFs in the network, we have $\mathbf{u}_i = Q_i\mathbf{x}$, where Q_i is a binary selection matrix, whose (j,k)-th element is 1 if x_k is the j-th input to node i, and 0 otherwise. When ribosomes are limited, the constant free ribosomes assumption used to derive (1) fails. Since the host cell produces a limited amount of ribosomes [3, 35], resource availability depends on the extent to which different nodes in the network demand them (see Figure 1B). We use z_T, z and z_i to denote the concentrations of total ribosomes, free ribosomes, and that of ribosomes bound to mRNA transcripts in node i, respectively. In particular, the ribosomes bound to node i depend on the free ribosome concentration (z), the concentration of mRNA transcripts in the node (m_i), and the binding affinity between them, which is characterized by the binding dissociation constant κ_i. Smaller κ_i indicates stronger capability of each mRNA molecule to bind free ribosomes. Specifically, from reaction rate equations, we can obtain $z_i = zm_i/\kappa_i$. Therefore, the concentration of ribosomes follows the conservation law [3]

$$z_T = z + \sum_{i=1}^{n} z_i = z \cdot (1 + \sum_{i=1}^{n} m_i/\kappa_i), \tag{3}$$

indicating that the total ribosome concentration is the summation of its free concentration (z) and its concentration bound in the nodes (z_i). From equation (3), the free concentration of ribosomes z can be found as

$$z = \frac{z_T}{1 + \sum_{i=1}^{n} m_i/\kappa_i}, \tag{4}$$

and by replacing the constant free ribosome concentration in (1) with the state-dependent amount derived in (4), the node dynamics in (1) can be modified as

$$\dot{m}_i = T_i F_i(\mathbf{u}_i) - \delta_i m_i, \qquad \dot{x}_i = R_i \frac{m_i/\kappa_i}{1 + m_i/\kappa_i + \sum_{j\neq i} m_j/\kappa_j} - \gamma_i x_i. \tag{5}$$

In the next section, we study the practical implications of model (5). In particular, we demonstrate that the model implies that, in addition to regulatory interactions, hidden interactions arise due to ribosome competition in GRNs.

3 Hidden interactions and effective interaction graphs

Synthetic biologists often analyze and design genetic circuits based on interaction graphs, which use directed edges to represent regulatory interactions among nodes. In a standard interaction graph, we draw $\mathrm{x_j} \rightarrow \mathrm{x_i}$ if TF $\mathrm{x_j}$ activates production of $\mathrm{x_i}$, and we draw $\mathrm{x_j} \dashv \mathrm{x_i}$ if TF $\mathrm{x_j}$ represses production of $\mathrm{x_i}$. In this section, we expand the concept of interaction graph to incorporate hidden interactions due to resource

competition. We call the resultant graph the *effective interaction graph*. We then provide simple rules to draw the effective interaction graphs, and illustrate their applications to predict the behavior of three simple GRNs.

Since an interaction graph represents the interactions among TFs in a GRN and since mRNA dynamics are often much faster than those of the TFs [1, 12], we set the mRNA dynamics in (5) to quasi-steady state [1, 12] to obtain:

$$\dot{x}_i = \underbrace{\frac{\bar{T}_i F_i(\mathbf{u}_i)}{1 + J_i F_i(\mathbf{u}_i) + \sum_{k \neq i} J_k F_k(\mathbf{u}_k)}}_{G_i(\mathbf{x}):\text{node } i \text{ effective production rate}} - \gamma_i x_i, \tag{6}$$

where parameter $\bar{T}_i := R_i T_i / \delta_i \kappa_i$ represents the maximum protein production rate and parameter $J_i := T_i / \delta_i \kappa_i$ represents the resource sequestration capability in node i, which we call its *resource demand coefficient*.

The effective production rate of node i, $G_i(\mathbf{x})$, encapsulates the joint effects of regulatory interactions and hidden interactions due to resource competition. While regulatory interaction on node i is characterized by $F_i(\mathbf{u}_i)$, resource competition effects on the node is described by a common denominator $R(\mathbf{x}) := 1 + \sum_{i=1}^{n} J_i F_i(\mathbf{u}_i)$, which is not present in the standard model (1). In particular, the *regulatory interaction* from $\mathrm{x_j}$ to $\mathrm{x_i}$ is determined by $\mathrm{sign}(\partial F_i / \partial x_j)$. If $\mathrm{sign}(\partial F_i / \partial x_j) > 0$, then the regulatory interaction is an activation ($\mathrm{x_j} \to \mathrm{x_i}$); if $\mathrm{sign}(\partial F_i / \partial x_j) < 0$, then the regulatory interaction is a repression ($\mathrm{x_j} \dashv \mathrm{x_i}$). We define *hidden interaction* due to resource competition from $\mathrm{x_j}$ to any node $\mathrm{x_i}$ to be determined by $\mathrm{sign}(\partial R / \partial x_j)$. Specifically, since $R(\mathbf{x})$ appears in the denominator of $G_i(\mathbf{x})$, it is a hidden activation ($\mathrm{x_j} \to \mathrm{x_i}$) if $\mathrm{sign}(\partial R / \partial x_j) < 0$, and a hidden repression ($\mathrm{x_j} \dashv \mathrm{x_i}$) if $\mathrm{sign}(\partial R / \partial x_j) > 0$.

The *effective interaction* from node j to node i is determined based on $\mathrm{sign}(\partial G_i / \partial x_j)$, representing how $\mathrm{x_j}$ affects the production rate of $\mathrm{x_i}$. In particular, we draw $\mathrm{x_j} \to \mathrm{x_i}$ (effective activation) if $\mathrm{sign}(\partial G_i / \partial x_j) > 0$, and we draw $\mathrm{x_j} \dashv \mathrm{x_i}$ (effective repression) if $\mathrm{sign}(\partial G_i / \partial x_j) < 0$. We draw $\mathrm{x_j} \multimap \mathrm{x_i}$ if $\mathrm{sign}(\partial G_i / \partial x_j)$ is undetermined, that is, it depends on parameters and/or the steady state the network is operating at.

Based on (6), we derive a set of graphical rules to determine the effective interaction originating from $\mathrm{x_j}$ to $\mathrm{x_i}$, based on regulatory interactions originating from $\mathrm{x_j}$. These graphical rules are summarized in Figure 2, and stated as follows.

1. If $\mathrm{x_j}$ has only one target $\mathrm{x_i}$, then the nature of effective interaction from $\mathrm{x_j}$ to $\mathrm{x_i}$ (i.e. activation vs. repression) is identical to the regulatory interaction. However, the strength of such interaction is weakened compared to that predicted by a standard model (see Figure 2A).
2. If $\mathrm{x_j}$ has multiple targets, then the effective interaction from $\mathrm{x_j}$ to its targets are undetermined (see Figure 2B).
3. If $\mathrm{x_i}$ is not a target of $\mathrm{x_j}$, and $\mathrm{x_j}$ is an activator (repressor), then $\mathrm{x_j}$ is effectively repressing (activating) $\mathrm{x_i}$ (see Figure 2C).

As application examples of the graphical rules, we determine the effective interaction graphs of three simple GRNs shown in Figure 3. Figure 3A shows a simple

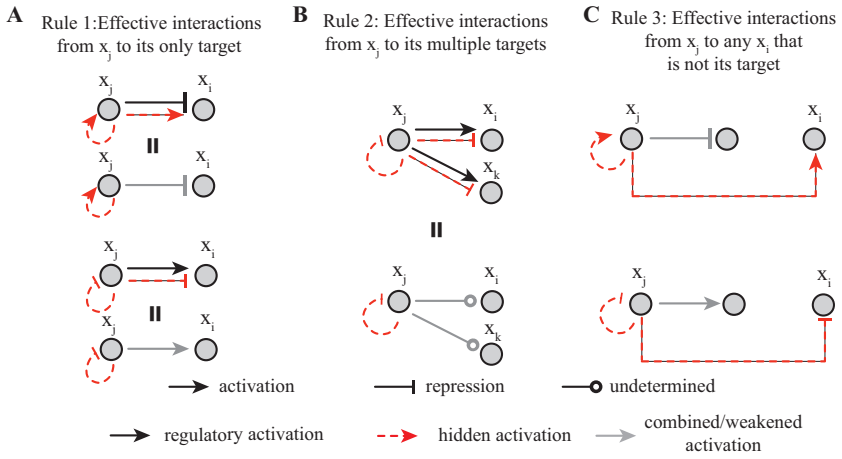

Fig. 2 Three graphical rules to draw effective interaction graph of any GRN with resource limitations. Black solid edges represent regulatory interactions, red dashed edges represent hidden interactions due to resource competition. If a black and a red edge have the same head and tail, we indicate their combined effects with a gray edge.

single-input motif [1], where a single TF input u represses two downstream targets x_1 and x_2. If we assume there is no resource competition, the steady state output of both x_1 and x_2 should decrease with u. However, in resource-limited cells, according to rule 2, the effective interactions from u to its targets are undetermined. A simulation example is presented in Figure 3A, where we show that steady state x_1 indeed increases with u for low concentrations of u. Physically, such unexpected behavior is due to the fact that as u increases to repress x_2, ribosomes bound to node 2 are released to effectively facilitate production of x_1, increasing its concentration.

In Figure 3B-C, we compare two additional examples of a two-stage activation cascade and a two-stage repression cascade. While the two networks have interchangeable functions of signal transduction and amplification [1], the former is more susceptible to resource competition. While the steady state input/output (i/o) response of an activation cascade can be entirely re-shaped by the hidden interactions (Figure 3B), that of a repression cascade increases monotonically in the presence of resource competition (Figure 3C). This result implies that certain network topologies may be more robust than others to resource competition. The robustness of a repression cascade to resource competition is due to the fact that both regulatory interactions ($u \dashv x_1 \dashv x_2$) and the hidden interaction ($u \rightarrow x_2$) increases output x_2 as input u increases.

In [27, 28], we demonstrate that in an activation cascade, the strength of the hidden interaction $u \dashv x_2$ can be tuned by changing the resource demand coefficient of node 1 (J_1), resulting in monotonically decreasing, increasing or biphasic steady state i/o responses. Specifically, reducing J_1 restores the monotonically increasing steady state i/o response. These model predictions are experimentally validated in [28].

However, due to the global and nonlinear features of resource competition, for more complicated networks, optimizing design parameters becomes impractical. Furthermore, the effects of resource competition must be re-examined when additional nodes are added to the network, complicating the design process. Therefore, it is desirable to design a feedback controller that can automatically mitigate the effects of hidden interactions so that networks can be designed solely based on regulatory interactions, and additional nodes can be included in a "plug-and-play" fashion. In the next section, we formulate this problem as a network disturbance decoupling problem.

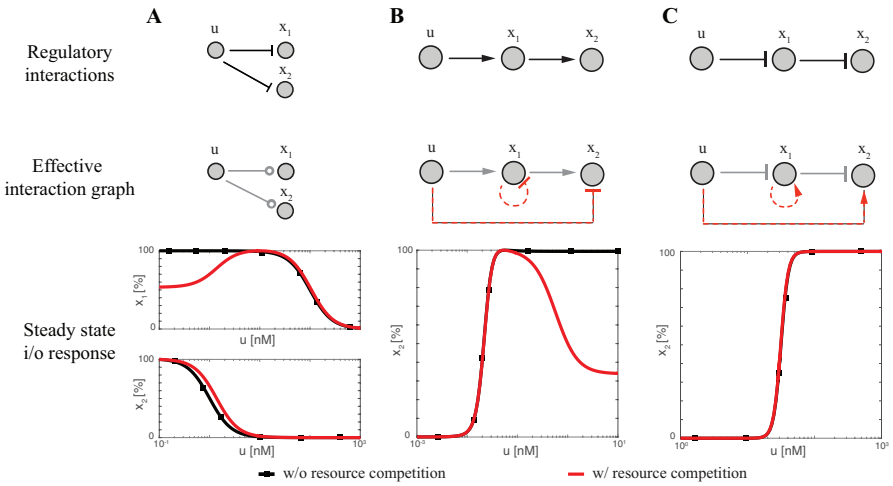

Fig. 3 Effects of resource competition on the steady state i/o responses of three example networks. (A): In a single-input motif, effective interactions from u to its targets become undetermined due to resource competition. Specifically, steady state i/o response from u to x_1 is biphasic. (B): Steady state i/o response of a genetic activation cascade may become biphasic due to hidden interactions arising from resource competition. Experimental results can be found in [28]. (C):Steady state i/o response of a repression cascade is guaranteed to be monotonically increasing since both regulatory interactions (black solid edges $u \dashv x_1 \dashv x_2$) and the hidden interaction due to resource competition (red dashed edge $u \rightarrow x_2$) increases output x_2 as input u increases. In all subfigures, steady state i/o responses with resource competition are simulated according to model (5), and steady state i/o responses without resource competition are simulated according to model (5) assuming disturbance inputs $w_i = \sum_{j \neq i} m_j / \kappa_j = 0$ for all i. Simulation parameters are listed in Table 1.

4 Mitigation of hidden interactions through network disturbance decoupling

The main difference between model (5) and the standard model in (1) is that in the standard model, gene expression in node i only depends on its own TF input $\mathbf{u}_i$,

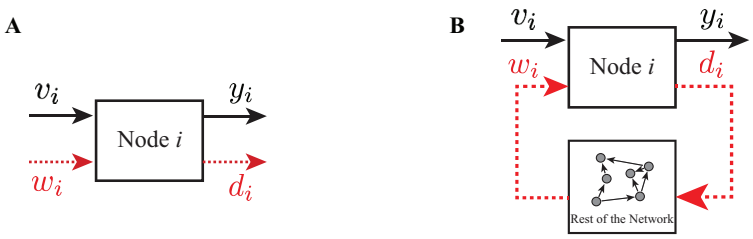

Fig. 4 (A): Each node i in a GRN with resource competition can be treated as a two-input-to-output system. Black edges represent reference input/outputs due to transcriptional regulations, and red dashed edges represent disturbances due to ribosome competition. (B): In a network setting, disturbance input to node i (w_i) is produced by resource demand by the rest of the network; resource demand of node i (d_i) becomes disturbance inputs to the rest of the network.

while in (5), it depends on the mRNA concentrations of other nodes ($m_j,\ j \neq i$). With reference to Figure 4A, according to model (5), each node in the network can be regarded as a two-input-two-output system. It takes a reference input $v_i := F_i(\mathbf{u}_i)$ and a disturbance input

$$w_i := \sum_{j \neq i} m_j / \kappa_j, \tag{7}$$

which characterizes how resource demands by the rest of the network affect dynamics of node i. Node i produces a reference output $y_i := x_i$ and a disturbance output

$$d_i := m_i / \kappa_i, \tag{8}$$

which quantifies resource demand by node i. Based on our definition of disturbance input (7) and disturbance output (8), resource competition creates another layer of interconnections among nodes in addition to regulatory interactions (see Figure 4B). Specifically, the disturbance input of each node is the summation of disturbance outputs of the other nodes in the network:

$$w_i = \sum_{j \neq i} d_j. \tag{9}$$

We would like that the steady state reference output of each node (y_i) to be only dependent on its own reference input (v_i) and essentially independent of disturbances among them (w_i). This concept, which we call *static network disturbance decoupling*, is demonstrated in Figure 5 and described as follows.

We consider a GRN where the steady state i/o responses of each node are parametrized by a small parameter ε, and can be written as:

$$y_i = h_i(v_i, w_i, \varepsilon), \qquad d_i = g_i(v_i, w_i, \varepsilon). \tag{10}$$

Functions $h_i(\cdot)$ and $g_i(\cdot)$ are twice continuously differentiable in ε for $(v_i, w_i, \varepsilon) \in \mathcal{V}_i \times \mathcal{W}_i \times (-\varepsilon^*, \varepsilon^*)$ with $\mathcal{V}_i \times \mathcal{W}_i \subseteq \mathbb{R}^2_+$, and $0 < \varepsilon^* \ll 1$. We further assume that

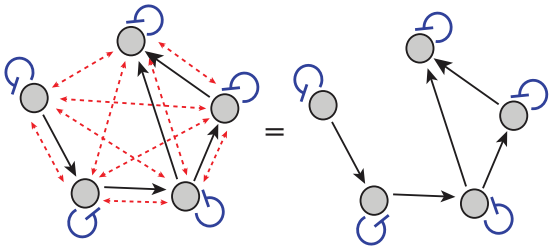

Fig. 5 In a network with disturbance decoupling property, steady state output of each node depends only on its reference input (black solid edges), and the steady state behavior of the network is essentially the same as that of a network without any disturbance (red dashed edges). Network disturbance decoupling can be achieved, for example, by implementing decentralized feedback controllers in the nodes (blue solid edges).

each node is a positive i/o system such that for all $v_i, d_i > 0$, we have $y_i, w_i > 0$. We use the following notations: $\mathbf{V} := \mathcal{V}_1 \times \cdots \times \mathcal{V}_n$, $\mathbf{W} := \mathcal{W}_1 \times \cdots \times \mathcal{W}_n$, $\mathbf{v} := [v_1, \cdots, v_n]^T$, $\mathbf{w} := [w_1, \cdots, w_n]^T$, $\mathbf{y} := [y_1, \cdots, y_n]^T$ and $\mathbf{d} := [d_1, \cdots, d_n]^T$.

Definition 1. (Network disturbance decoupling.) A network is said to have *local ε-static network disturbance decoupling property* in $\mathcal{V} \times \tilde{\mathcal{W}}$ if there exists an ε^* sufficiently small and an open set $\tilde{\mathcal{W}} \subseteq \mathbf{W}$ such that for all $i = 1, \cdots, n$,

$$y_i = h_i(v_i, w_i(\mathbf{v}, \varepsilon), \varepsilon) = h_i(v_i, 0, 0) + \mathcal{O}(\varepsilon). \tag{11}$$

In principle, network disturbance decoupling requires each node to possess some disturbance attenuation property. In addition, since disturbance input to each node $w_i = w_i(\mathbf{v}, \varepsilon)$ depends on resource demand by the rest of the network, we need to ensure that w_i is not amplified while we increase disturbance attenuation capability in each node. In what follows, we give algebraic conditions on the node and the network such that static network disturbance decoupling can be achieved. We first state the definition of *ε-static disturbance attenuation*, which is the property required for the reference output of each node in isolation to be essentially independent of its disturbance input.

Definition 2. (Node disturbance attenuation.) Node i has ε-static disturbance attenuation property in $\mathcal{V}_i \times \mathcal{W}_i$ if $h_i(v_i, w_i, 0) = h_i(v_i, 0, 0)$ for all $(v_i, w_i) \in \mathcal{V}_i \times \mathcal{W}_i$.

For a node with ε-static disturbance attenuation property, the effect of disturbance input on reference output is attenuated by a factor of ε, and can be written as $y_i = h_i(v_i, 0, 0) + \mathcal{O}(\varepsilon)$ for ε sufficiently small. This property does not require any information on the network, and is a characterization of each node in isolation. It can be achieved, for example, by implementing decentralized controllers in the nodes. When node i is part of the network, since w_i also depends on ε, it may grow unbounded as $\varepsilon \to 0$, in principle. The next property on the network excludes this possibility and guarantees that w_i is smooth in ε as $\varepsilon \to 0$.

Definition 3. (Network ε-well-posedness.) Consider a network where the nodes are connected according to (9), and the steady state i/o response of each node follows (10). It is *locally ε-well-posed* in $\mathcal{V}\times\mathcal{W}\subseteq\mathbf{V}\times\mathbf{W}$ if there is an open set $\mathcal{W}\subseteq\mathbf{W}$ and $\varepsilon^*>0$ such that there exists $\mathbf{w}(\mathbf{v},\varepsilon)\in\mathcal{W}$ that satisfies

$$w_i=\sum_{j\neq i}g_j(v_j,w_j,\varepsilon),\text{for all } i\in\{1,\cdots,n\}. \tag{12}$$

Furthermore, $\mathbf{w}(\mathbf{v},\varepsilon)$ is continuously differentiable in ε for all $(\mathbf{v},\mathbf{w},\varepsilon)\in\mathcal{V}\times\mathcal{W}\times(-\varepsilon^*,\varepsilon)$.

The following result provides sufficient conditions for local ε-static network disturbance decoupling (see [29] for details).

Theorem 1. *A network has local ε-static network disturbance decoupling property in $\mathcal{V}\times\mathcal{W}$ if (1) each node i has ε-disturbance attenuation property in $\mathcal{V}_i\times\mathcal{W}_i$, and (2) the network is locally ε-well-posed in $\mathcal{V}\times\mathcal{W}$.*

While condition (1) in Theorem 1 can be obtained by implementing decentralized controllers in the nodes, condition (2) needs to be certified by exploring more properties of the network. We further assume that when $\varepsilon=0$, steady state disturbance output of each node (d_i) is affine in its disturbance input (w_i) for all $(\mathbf{v},\mathbf{w})\in\mathcal{V}\times\mathcal{W}$

$$g_i(v_i,w_i,0)=\bar{g}_i(v_i)+\hat{g}_i(v_i)w_i. \tag{13}$$

In this case, the local ε-well-posedness property of a network can be certified by the diagonal dominance of an interconnection matrix A, whose (j,k)-th element is defined as

$$A_{(j,k)}(\mathbf{v}):=\begin{cases}1, & \text{if } j=k,\\ -\hat{g}_k(v_k), & \text{if } j\neq k.\end{cases} \tag{14}$$

This result is stated in the following theorem, and we refer the readers to [29] for detailed proofs and discussions. Note that the positivity of i/o signals implies that $\bar{g}_i(v_i),\hat{g}_i(v_i)$ must be positive.

Theorem 2. *Assume that the steady state disturbance i/o response of each node i follows (13) and that the nodes are connected according to (9). If the interconnection matrix defined in (14) is diagonally dominant for all $\mathbf{v}\in\mathcal{V}$, then there exists an open set $\mathcal{W}$ such that the network is locally ε-well-posed in $\mathcal{V}\times\mathcal{W}$.*

Since all diagonal elements in A are positive and all off-diagonal elements are negative, a direct consequence of Theorem 2 is that as the number of nodes in the network increases, the set of admissible reference inputs $\mathcal{V}$ such that the interconnection matrix A remain diagonally dominant shrinks in size.

Note that the diagonal dominance condition in Theorem 2 resembles a network small-gain theorem for stability test [34]. However, in the context of [34], the elements in the interconnection matrix are dynamic i/o gains of the individual nodes,

while here, the elements in interconnection matrix A are steady state i/o gains. Therefore, instead of guaranteeing stability, Theorem 2 guarantees, roughly speaking, that a steady state of the network remains $\mathcal{O}(1)$ as $\varepsilon \to 0$. In the next section, we propose a biomolecular feedback controller design that guarantees ε-static network disturbance decoupling of the resource competition network. We then study its stability in Section 6.

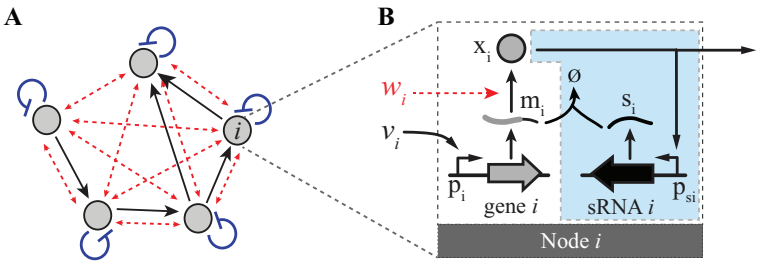

Fig. 6 (A): Decentralized implementation of sRNA-based feedback controllers in a GRN. (B): Biomolecular mechanism of the controller, where elements of the controller are shaded in blue.

5 Biomolecular realization of disturbance decoupling through decentralized sRNA-based feedback

Small RNAs (sRNAs) are short non-coding RNAs that can bind to complementary RNAs to induce their rapid degradation [20]. Recently, they have been identified as critical gene regulators in nature. For example, negative feedback systems using sRNA have been identified in iron homeostasis [21], quorum sensing [33] and sugar metabolism [18]. In this section, we demonstrate that decentralized sRNA-based feedback controllers (Figure 6) can achieve ε-static network disturbance decoupling. We first introduce the biomolecular mechanism of this controller and then show that each node has ε-static disturbance attenuation property and the resulting network is ε-well-posed.

A diagram of node i equipped with the proposed sRNA-based feedback is shown in Figure 6B. In node i, the output protein x_i transcriptionally activates production of sRNA s_i, which binds with the mRNA m_i to form a complex which then degrades rapidly [21]. When ribosome availability decreases, less x_i is produced, resulting in reduced production of s_i, which in turn increases mRNA concentration to compensate for reduction in ribosome concentration. Based on reaction rate equations [20], an ODE model of each node i can be written as follows:

$$\begin{aligned}
\dot{m}_i &= GT_i v_i - \delta m_i - G m_i s_i/k_i,\\
\dot{s}_i &= GT_{si}\frac{x_i/k_{si}}{1+x_i/k_{si}} - \delta s_i - G m_i s_i/k_i,\\
\dot{x}_i &= R_i\frac{m_i/\kappa_i}{1+m_i/\kappa_i+w_i} - \gamma x_i,
\end{aligned} \tag{15}$$

where m_i, s_i and x_i each represents the concentration of mRNA, sRNA and TF output in node i. Recall from (7)-(8) that disturbance input $w_i = \sum_{j\neq i} m_j/\kappa_j$ and reference input $v_i = F_i(\mathbf{u}_i)$, where $F_i(\mathbf{u}_i)$ represents regulatory interactions. In (15), δ and γ are the decay rate constants of mRNAs and proteins, respectively, which we have assumed to be the same for all nodes without loss of generality; k_i and k_{si} are dissociation constants characterizing mRNA-sRNA binding, and the binding of $\mathrm{x_i}$ with the sRNA promoters, respectively; κ_i is the dissociation constant of free ribosomes with RBS of $\mathrm{m_i}$, and G represents the rapid degradation of the mRNA-sRNA complex. To compensate for the decrease in gene expression due to rapid degradation (G) of mRNA and sRNA, we set their transcription rates (GT_i and GT_{si}) to scale with G. This can be implemented physically by increasing the DNA amount of the gene and the sRNA. By letting $\varepsilon := \delta/G$, the steady state of (15) can be found to be:

$$\begin{aligned}
m_i &= \frac{T_i\kappa_i k_{si}\gamma v_i(1+w_i)}{T_{si}R_i - (\gamma k_{si}+R_i)T_i v_i} + \mathcal{O}(\varepsilon),\\
s_i &= \frac{T_{si}R_i - (\gamma k_{si}+R_i)T_i v_i}{\kappa_i k_{si}\gamma(1+w_i)} + \mathcal{O}(\varepsilon),\\
x_i &= \frac{T_i k_{si} v_i}{T_{si}-T_i v_i} + \mathcal{O}(\varepsilon),
\end{aligned} \tag{16}$$

when the reference input v_i belongs to the *node admissible input set* $\mathcal{V}_i$:

$$\mathcal{V}_i = \left\{ v_i : 0 < v_i < \frac{T_{si}R_i}{T_i(\gamma k_{si}+R_i)} \right\}. \tag{17}$$

Since the zero-th order approximation of steady state output x_i in (16) is independent of disturbance input w_i, node i has ε-disturbance attenuation property for all $v_i \in \mathcal{V}_i$ and w_i positive. To verify if the GRN with decentralized sRNA-based controllers is locally ε-well-posed, we note that the steady state disturbance output of node i is:

$$d_i = \frac{m_i}{\kappa_i} = \frac{T_i k_{si}\gamma v_i(1+w_i)}{T_{si}R_i - (\gamma k_{si}+R_i)T_i v_i} + \mathcal{O}(\varepsilon), \tag{18}$$

which is affine in the disturbance input w_i when $\varepsilon = 0$. This satisfies the assumption in (13) with

$$\hat{g}_i(v_i) = \frac{T_i k_{si}\gamma v_i}{T_{si}R_i - (\gamma k_{si}+R_i)T_i v_i}.$$

Therefore, according to Theorem 2, the network is ε-well-posed in a *network admissible input set* $\mathcal{V}$, in which the interconnection matrix defined according to (14) is diagonally dominant for all $\mathbf{v} \in \mathcal{V}$. Specifically, we can write

$$\mathcal{V} := \left\{ \mathbf{v} \in \mathbf{V} : \sum_{j \neq i} \hat{g}_j(v_j) < 1, \forall i = 1, \cdots, n \right\}. \tag{19}$$

Hence, due to Theorem 1, the network has the ε-disturbance decoupling property if the reference inputs satisfy $\mathbf{v} \in \mathcal{V}$. This implies that steady state output of each node i in the GRN tracks its reference input v_i, and becomes essentially decoupled from resource demand by the rest of the network. Note that as we discussed in the Section 4, according to (19), since $\hat{g}_j(v_j)$ is positive for each $v_i \in \mathcal{V}_i$, the size of the admissible input set of the resource competition network shrinks as more nodes are added to the node. This is a major trade-off of this decentralized feedback design.

6 Stability of decentralized sRNA-based feedback

In the previous section, we demonstrate that the steady state output of each node depends essentially only on its own reference input (v_i) as long as the reference inputs fall into the admissible input set ($\mathbf{v} \in \mathcal{V}$). However, these results do not imply stability of the corresponding network steady state. To study stability, we consider a special case where the network is homogeneous such that parameters of and the external reference input to each node are identical. We further assume that there is no regulatory interaction among nodes (Fig.7) so that we do not account for instability, if any, due to regulatory interactions. Let $\mathbf{x}_i := [m_i, s_i, x_i]^T$ be the states of node i, one steady state of the network lies on the diagonal of the $3n$-dimensional space: $\mathbf{x}^* = [\mathbf{x}_1^{*T}, \cdots, \mathbf{x}_n^{*T}]^T$ with $\mathbf{x}_1^* = \cdots = \mathbf{x}_n^*$. Here, through linearization, we demonstrate that network steady state $\mathbf{x}^*$ is indeed locally asymptotically stable.

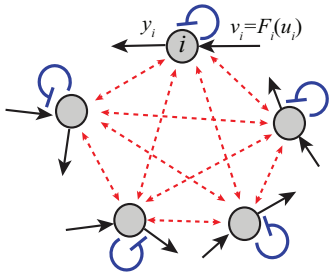

Fig. 7 Homogeneous GRN with decentralized feedback controllers and resource competition for stability certification. Each node i takes an external reference input v_i and is equipped with an sRNA-based feedback controller (blue solid edges). The nodes are connected by hidden interactions arising from resource competition (red dashed edges).

To this end, we leverage the following network stability result from vehicle formation control [15]. Consider a network consists of N identical linear time-invariant nodes, dynamics of each node i are described by

$$\dot{\eta}_i = P_A\eta_i + P_B u_i, \qquad \zeta_i = P_{C1}\eta_i, \qquad \psi_{ij} = P_{C2}(\eta_i - \eta_j),\ j \in \mathcal{J}_i, \tag{20}$$

where $\eta_i \in \mathbb{R}^m$ are the states of the node, u_i is the input, ζ_i and ψ_{ij} are the absolute and relative measurements, respectively, and $\mathcal{J}_i \subseteq \{1,\cdots,N\}\setminus\{i\}$ represents the set of nodes that communicate with node i. P_A, P_B, P_{C1} and P_{C2} are constant matrices with appropriate dimensions. The communication scheme defines a directed graph of the network, whose Laplacian $\mathcal{L}$ is defined as

$$\mathcal{L}_{(i,i)} = 1, \qquad \mathcal{L}_{(i,j)} = \begin{cases} -\frac{1}{|\mathcal{J}_i|},\ j \in \mathcal{J}_i, \\ 0, \qquad j \notin \mathcal{J}_i. \end{cases} \tag{21}$$

We assume that the following decentralized controller is applied to each node i:

$$\dot{\theta}_i = K_A\theta_i + K_{B1}\zeta_i + K_{B2}\psi_i, \qquad u_i = K_C\theta_i + K_{D1}\zeta_i + K_{D2}\psi_i, \tag{22}$$

where

$$\psi_i = \frac{1}{|\mathcal{J}_i|}\sum_{j\in\mathcal{J}_i}\psi_{ij}, \tag{23}$$

and $\theta_i \in \mathbb{R}^p$ are the controller states. K_A, K_{B1}, K_{B2}, K_C, K_{D1} and K_{D2} are constant matrices with appropriate dimensions. The following result converts the stability problem of the network, which is an $N\times(m+p)$-dimensional system, into stability problems of N disconnected $(m+p)$-dimensional systems.

Theorem 3. *[15] Decentralized controllers (22) stabilize the network if and only if the following matrices (24) are Hurwitz for all N eigenvalues ($\lambda_1,\cdots,\lambda_N$) of $\mathcal{L}$:*

$$\begin{bmatrix} P_A + P_B K_{D1} P_{C1} + \lambda_l P_B K_{D2} P_{C2} & P_B K_C \\ K_{B1} P_{C1} + \lambda_l K_{B2} P_{C2} & K_A \end{bmatrix},\ l = 1,\cdots,N. \tag{24}$$

Applying Theorem 3 to a GRN connected through ribosome competition significantly reduces the technical difficulties in network stability certification. In particular, since disturbance input to each node i follows $w_i = \sum_{j\neq i} m_j/\kappa_j$, the resultant directed graph of the network is a complete graph, with graph Laplacian

$$\mathcal{L} = \begin{bmatrix} 1 & -\frac{1}{n-1} & -\frac{1}{n-1} & \cdots & -\frac{1}{n-1} \\ -\frac{1}{n-1} & 1 & -\frac{1}{n-1} & \cdots & -\frac{1}{n-1} \\ \vdots & \vdots & \vdots & \ddots & \vdots \\ -\frac{1}{n-1} & -\frac{1}{n-1} & -\frac{1}{n-1} & \cdots & 1 \end{bmatrix}. \tag{25}$$

The eigenvalues of $\mathcal{L}$ are

$$\lambda_1 = 0 \qquad \text{and} \qquad \lambda_2 = n/(n-1) \quad \text{(repeated)}. \tag{26}$$

Therefore, by linearizing the network at steady state $\mathbf{x}^*$, its local stability can be certified by stability of 2 lower dimensional subsystems. In particular, linearizing (15) results in the following linearized node dynamics

$$\begin{aligned} \dot{m}_i &= -(Gs_i^*/k_i + \delta)m_i - Gm_i^* s_i/k_i, \\ \dot{s}_i &= GT_{si} f_{si} x_i - Gs_i^* m_i/k_i - (Gm_i^*/k_i + \delta)s_i, \\ \dot{x}_i &= R_i q_{ii} m_i + R_i \sum_{j\neq i} q_{ij} m_j - \gamma x_i, \end{aligned} \tag{27}$$

where we have defined

$$f_{si} := \frac{\mathrm{d}}{\mathrm{d}x_i} \frac{x_i/k_{si}}{1 + x_i/k_{si}}\bigg|_{\mathbf{x}^*} = \frac{1/k_{si}}{(1 + x_i^*/k_{si})^2}, \tag{28}$$

$$q_{ii} := \frac{\partial}{\partial m_i} \frac{m_i/\kappa_i}{1 + m_i/\kappa_i + \sum_{j\neq i} m_j/\kappa_j}\bigg|_{\mathbf{x}^*} = \frac{(1 + \sum_{j\neq i} m_j^*/\kappa_j)/\kappa_i}{(1 + m_i^*/\kappa_i + \sum_{j\neq i} m_j^*/\kappa_j)^2}, \tag{29}$$

$$q_{ij} := \frac{\partial}{\partial m_j} \frac{m_i/\kappa_i}{1 + m_i/\kappa_i + \sum_{j\neq i} m_j/\kappa_j}\bigg|_{\mathbf{x}^*} = -\frac{m_i^*/\kappa_i\kappa_j}{(1 + m_i^*/\kappa_i + \sum_{j\neq i} m_j^*/\kappa_j)^2}. \tag{30}$$

System (27) can be put into the form in Theorem 3. Specifically, we take

$$\eta_i = \begin{bmatrix} m_i, \\ s_i \end{bmatrix}, \qquad \theta_i = x_i, \qquad P_A = \begin{bmatrix} -Gs_i^*/k_i - \delta & -Gm_i^*/k_i \\ -Gs_i^*/k_i & -Gm_i^*/k_i - \delta \end{bmatrix},$$

$$P_B = \begin{bmatrix} 0 \\ GT_{si} f_{si} \end{bmatrix}, \quad P_{C1} = \begin{bmatrix} 1 & 0 \end{bmatrix}, \qquad P_{C2} = \begin{bmatrix} -R_i q_{ij} & 0 \end{bmatrix},$$

$$K_A = -\gamma, \qquad K_C = 1, \qquad K_{D1} = 0,$$

$$K_{D2} = 0, \qquad K_{B1} = R_i[q_{ii} + (n-1)q_{ij}], \quad K_{B2} = n-1.$$

Using (26), Theorem 3 implies that stability of the network can be implied by demonstrating that the following two matrices A^1_{equiv} and

$$A^2_{\text{equiv}}$$

, each corresponding to $\lambda_1 = 0$ and $\lambda_2 = n/(n-1)$, are Hurwitz:

$$A^1_{\text{equiv}} = \begin{bmatrix} -Gs_i^*/k_i - \delta & -Gm_i^*/k_i & 0 \\ -Gs_i^*/k_i & -Gm_i^*/k_i - \delta & GT_{si} f_{si} \\ R_i[q_{ii} + (n-1)q_{ij}] & 0 & -\gamma \end{bmatrix}, \tag{31}$$

and

$$A^2_{\text{equiv}} = \begin{bmatrix} -Gs_i^*/k_i - \delta & -Gm_i^*/k_i & 0 \\ -Gs_i^*/k_i & -Gm_i^*/k_i - \delta & GT_{si} f_{si} \\ R_i(q_{ii} - q_{ij}) & 0 & -\gamma \end{bmatrix}. \tag{32}$$

Assume that the reference inputs are within the admissible reference input set $\mathcal{V}$, by substituting in the steady states found in (16) and using Routh-Hurwitz condition, both matrices can be found Hurwitz, showing that a homogeneous network composed of decentralized sRNA-based feedback controllers is stable when $\mathbf{v} \in \mathcal{V}$.

7 Application examples

Here, we apply the decentralized sRNA-based feedback controllers to two GRNs of Figure 3. Both networks failed to perform as expected due to hidden interactions arising from resource competition. In Figure 8, we simulate the steady state i/o responses of the single-input motif (Figure 8A) and the activation cascade (Figure 8B) equipped with decentralized feedback controllers described in Section 5. Consistently with our predictions, as G increases (i.e. ε decreases), the steady state i/o responses of the networks become closer to the hypothetical case where disturbance inputs to all nodes are assumed to zero (i.e. $w_i = \sum_{j \neq i} m_j / \kappa_j = 0$ for all i). These simulations support our claim that decentralized sRNA-based feedback can increase network's robustness to resource competition. We envision that with the decentralized controllers, GRNs with increased size and complexity can be constructed in a modular fashion, bringing synthetic biology one step closer to real-world applications.

8 Discussion and conclusions

In this paper, we review our recent research outcomes on the resource competition problem in genetic circuits. We demonstrate that resource competition creates hidden interactions among nodes, changing the intended topology of the circuit. To mitigate the effects of resource competition, we take a control theoretic perspective. We treat these hidden interactions as disturbances, and formulate a static network disturbance decoupling problem. In a network with network disturbance decoupling property, the reference output of each node depends essentially only on its own reference input, and not on the hidden interactions among nodes. We give algebraic conditions on node dynamics and on the network that guarantees disturbance decoupling, and demonstrate that these conditions can be obtained by decentralized sRNA-based feedback controllers *in vivo*. While these results are promising, we still need to tackle the case in which the inputs to the nodes are time-varying and the results we obtain are global instead of being local. These problems are particularly difficult due to the nonlinear and singular structure of the dynamics when feedback gains are increased. To the best of our knowledge, such peculiar structures do not have a counter-part in more traditional engineering systems. Therefore, a solution will likely require the development of novel control theoretic methods.

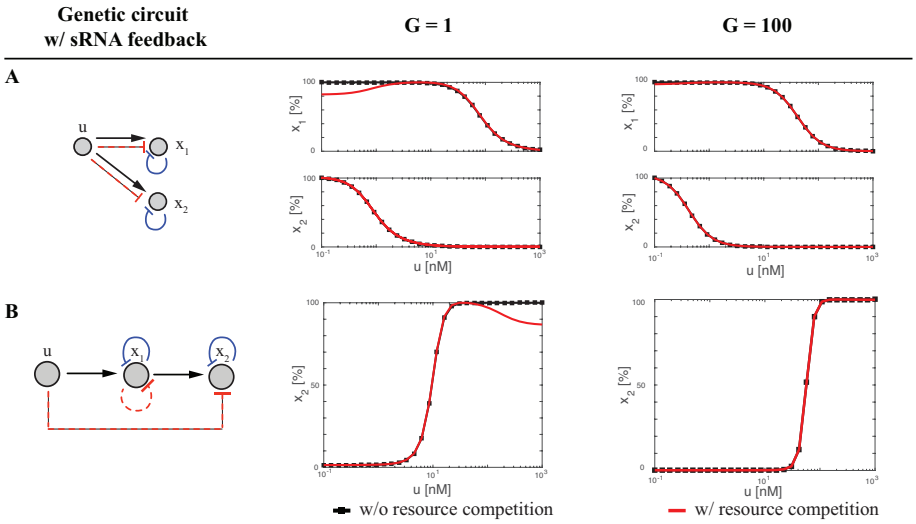

Fig. 8 Steady state i/o responses of the single-input motif (A) and the activation cascade (B) with different G values. In the network interaction graph, black solid edges represent transcriptional regulation, red dashed edges represent hidden interactions due to resource competition and blue solid edges represent sRNA-based feedback. We simulate the responses with resource competition using model (15) and $w_i = \sum_{j\neq i} m_j/\kappa_j$ (red solid lines). We further assume $w_i = 0$ for all i to obtain the steady state i/o responses without resource competition (black solid line with square markers). Simulation parameters are listed in Table 1.

Our results provide examples of how introducing systems and control concepts can help address concrete problems in synthetic biology. In general, synthetic biology is an exciting platform to leverage existing control theoretic tools and to introduce new ones. Due to various sources of uncertainties and disturbances present in living cells, the advancement of synthetic biology relies heavily on our capabilities to engineer robust, modular and scalable biomolecular systems. While such capabilities are still largely missing at this stage, they can be significantly improved by synthesizing feedback controllers in biomolecular systems.

Table 1 Simulation parameters ($i = 1, 2$)

	δ_i	γ_i	T_1	T_2	k_1	k_2	κ_1	κ_2	R_i	n_1	n_2	T_{s1}	T_{s2}	k_{si}	β_i
Unit	hr^{-1}	hr^{-1}	$\text{nM}\cdot\text{hr}^{-1}$	$\text{nM}\cdot\text{hr}^{-1}$	nM	nM	μM	μM	$\text{nM}\cdot\text{hr}^{-1}$	-	-	nM^2	nM^2	nM	-
Figure 3A	10	1	10^3	10^3	10^2	1	10^3	10^2	10^3	2	2	-	-	-	-
Figure 3B	5	1	10^3	10^2	1	2	10^2	10^3	10^3	2	4	-	-	-	10^{-3}
Figure 3C	5	1	10^3	10^2	1	2	10^2	10^3	10^3	2	4	-	-	-	-
Figure 8A	10	1	10^3	10^3	10^2	1	10^3	10^2	10^3	2	2	1200	1200	10	-
Figure 8B	5	1	10^3	10^2	1	2	10^2	10^3	10^3	2	4	1200	120	10	10^{-3}

Acknowledgements We would like to thank Ms. Rushina Shah who assisted in the proof-reading of the manuscript. This work was supported by AFOSR grant FA9550-14-1-0060.

References

1. U. Alon. *An Introduction to Systems Biology: Design Principles of Biological Circuits*. Chapman & Hall/CRC Press, 2006.
2. L. T. Bereza-Malcolm, G. Mann, and A. E. Franks. Environmental sensing of heavy metals through whole cell microbial biosensors: A synthetic biology approach. *ACS Synth. Biol.*, 4(5):535–546, 2015.
3. H. Bremer and P. P. Dennis. Modulation of chemical composition and other parameters of the cell by growth rate. In F. C. Neidhardt, editor, *Escherichia coli and Salmonella: Cellular and Molecular Biology*. ASM Press, 1996.
4. D. E. Cameron, C. J. Bashor, and J. J. Collins. A brief history of synthetic biology. *Nat. Rev. Micro.*, 12(5):381–390, May 2014.
5. M. Carbonell-Ballestero, E. Garcia-Ramallo, R. Montañez, C. Rodriguez-Caso, and J. Macía. Dealing with the genetic load in bacterial synthetic biology circuits: convergences with the ohm's law. *Nucleic Acids Res.*, 44(1):496–507, 2015.
6. S. Cardinale and A. P. Arkin. Contextualizing context for synthetic biology- identifying causes of failure of synthetic biological systems. *Biotechnol. J.*, 7:856–866, 2012.
7. F. Ceroni, R. Algar, G.-B. Stan, and T. Ellis. Quantifying cellular capacity identifies gene expression designs with reduced burden. *Nat. Methods*, 12(5):415–422, 2015.
8. D. Chakravarti and W. W. Wong. Synthetic biology in cell-based cancer immunotherapy. *Trends Biotechnol.*, 33(8):449–461, 2015.
9. T. Danino, A. Prindle, G. A. Kwong, M. Skalak, H. Li, K. Allen, J. Hasty, and S. N. Bhatia. Programmable probiotics for detection of cancer in urine. *Sci. Transl. Med.*, 7(289):289ra84–289ra84, 2015.
10. D. Del Vecchio. Modularity, context-dependence, and insulation in engineered biological circuits. *Trends Biotechnol.*, 33(2):111–119, 2015.
11. D. Del Vecchio, A. J. Dy, and Y. Qian. Control theory meets synthetic biology. *J. R. Soc. Interface*, 13:20160380, 2016.
12. D. Del Vecchio and R. M. Murray. *Biomolecular Feedback Systems*. Princeton University Press, Princeton, 2014.
13. D. Del Vecchio, A. J. Ninfa, and E. D. Sontag. Modular cell biology: retroactivity and insulation. *Mol. Syst. Biol.*, 4(1), 2008.
14. M. B. Elowitz and S. Leibler. A synthetic oscillatory network of transcriptional regulators. *Nature*, 403(6767):335–338, 2000.
15. J. A. Fax and R. M. Murray. Graph laplacians and stabilization of vehicle formations. In *Proceedings of the 15th IFAC World Congress*, volume 35, pages 55–60, Barcelona, Spain, 2002.
16. T. S. Gardner, C. R. Cantor, and J. J. Collins. Construction of a genetic toggle switch in Escherichia coli. *Nature*, 403(6767):339–342, 2000.
17. A. Gyorgy, J. I. Jiménez, J. Yazbek, H.-H. Huang, H. Chung, R. Weiss, and D. Del Vecchio. Isocost lines describe the cellular economy of gene circuits. *Biophys. J.*, 109(3):639–646, 2015.
18. F. Kalamorz, B. Reichenbach, W. März, B. Rak, and B. Görke. Feedback control of glucosamine-6-phosphate synthase GlmS expression depends on the small RNA GlmZ and involves the novel protein YhbJ in Escherichia coli. *Mol. Microbiol.*, 65(6):1518–1533, 2007.
19. S. Klumpp, J. Dong, and T. Hwa. On Ribosome Load, Codon Bias and Protein Abundance. *PLoS One*, 7(11):e48542, 2012.
20. E. Levine, Z. Zhang, T. Kuhlman, and T. Hwa. Quantitative characteristics of gene regulation by small RNA. *PLoS Biol.*, 5(9):e229, 2007.

21. E. Massé, F. E. Escorcia, and S. Gottesman. Coupled degradation of a small regulatory RNA and its mRNA targets in *Escherichia coli*. *Genes & Development*, 17(19):2374–2383, 2003.
22. W. H. Mather, J. Hasty, L. S. Tsimring, and R. J. Williams. Translation cross talk in gene networks. *Biophys. J.*, 104:2564–2572, 2013.
23. D. Mishra, P. M. Rivera, A. Lin, D. Del Vecchio, and R. Weiss. A load driver device for engineering modularity in biological networks. *Nat. Biotechnol.*, 32:1268–1275, 2014.
24. K. S. Nilgiriwala, J. I. Jiménez, P. M. Rivera, and D. Del Vecchio. Synthetic tunable amplifying buffer circuit in *E. coli*. *ACS Synth. Biol.*, 4(5):577–584, 2015.
25. P. P. Peralta-Yahya, F. Zhang, S. B. del Cardayre, and J. D. Keasling. Microbial engineering for the production of advanced biofuels. *Nature*, 488:320–328, 2012.
26. P. E. M. Purnick and R. Weiss. The second wave of synthetic biology: from modules to systems. *Nat. Rev. Mol. Cell Biol.*, 10:410–422, 2009.
27. Y. Qian and D. Del Vecchio. Effective interaction graphs arising from resource limitations in gene networks. In *Proceedings of the 2015 American Control Conference (ACC)*, pages 4417–4423, Chicago, IL, 2015.
28. Y. Qian, H.-H. Huang, J. I. Jiménez, and D. Del Vecchio. Resource competition shapes the response of genetic circuits. *ACS Synth. Biol.*, 2017 (in press). DOI: 10.1021/acssynbio.6b00361.
29. Y. Qian and D. D. Vecchio. Mitigation of ribosome competition through distributed sRNA feedback. In *IEEE 55th Conference on Decision and Control (CDC)*, pages 758–763, Las Vegas, NV, 2016.
30. A. Raveh, M. Margaliot, E. D. Sontag, and T. Tuller. A model for competition for ribosomes in the cell. *J. R. Soc. Interface*, 13:20151062, 2015.
31. N. Rosenfeld and U. Alon. Response delays and the structure of transcription networks. *J. Mol. Biol.*, 329(4):645–654, 2003.
32. D. Siegal-gaskins, Z. A. Tuza, J. Kim, V. Noireaux, and R. M. Murray. Gene circuit performance characterization and resource usage in a cell- free 'breadboard'. *ACS Synth. Biol.*, 3:416–425, 2014.
33. K. C. Tu, T. Long, S. L. Svenningsen, N. S. Wingreen, and B. L. Bassler. Negative feedback loops involving small regulatory rnas precisely control the vibrio harveyi quorum-sensing response. *Mol. Cell*, 37(4):567–579, 2010.
34. M. Vidyasagar. *Input-output analysis of large-scale interconnected systems*, volume 29 of *Lecture Notes in Control and Information Sciences*. Springer-Verlag, New York, 1981.
35. J. Vind, M. A. Sørensen, M. D. Rasmussen, and S. Pedersen. Synthesis of proteins in Escherichia coli is limited by the concentration of free ribosomes: Expression from reporter gene does not always reflect functional mRNA levels. *J. Mol. Biol.*, 231:678–688, 1993.